Wear Behavior of Pb-Mo-S Solid Lubricating Coatings

K.J. Wahl, D.N. Dunn*, and I.L. Singer
Code 6176, Naval Research Laboratory, Washington DC 20375-5342
**Present Address: Dept. of Materials Science, University of Virginia, Charlottesville VA 22903.*

Abstract

Amorphous Pb-Mo-S coatings 200 to 510 nm thick were deposited by dual ion-beam deposition (IBD) onto steel and Si substrates. Coating wear studies were performed using ball-on-flat reciprocating sliding with steel ball counterfaces in dry air. Tests were run between 1 and 100000 sliding cycles, and wear depths measured by interference microscopy. Morphology and chemistry of the as-deposited coatings and worn surfaces were investigated with optical microscopy, micro-Raman spectroscopy and cross-section high resolution transmission electron microscopy (HRTEM). Pb-Mo-S coatings were found to be quite wear resistant; no more than 25% of the coating thickness was removed by 10000 sliding cycles. Two wear mechanisms were identified. At the nanometer scale, wear proceeded in a two-part process: transformation of the coating surface to MoS_2, then layer-by-layer removal of MoS_2. At the micrometer scale, wear occurred by plowing. The long endurance of Pb-Mo-S coatings was attributed to slow wear of the coatings, with lubricant redistribution processes playing a minor role.

Keywords: wear, molybdenum disulfide, solid lubrication, coatings

Accepted for publication in *Wear*:1/99

1. Introduction

Advances in solid lubrication by MoS_2 have been made by investigating the relationships between processing, microstructure, friction, wear and endurance. Studies of sputter deposited MoS_2 showed that coating microstructure plays a large role in both wear behavior and coating lifetime. For example, early sputter deposited MoS_2 coatings formed platelets having a columnar, edge oriented (basal plane perpendicular to substrate), porous microstructure [1]. Because of this structure, the coatings lost platelets through fracture during sliding [2] as well as deformed by tilting or bending of columnar platelets [3-5], as observed by scanning electron microscopy. Fleischauer and co-workers [4, 5] used x-ray diffraction (XRD) to confirm and quantify reorientation after sliding. Hilton et al. [6] later showed that the degree of reorientation is dependent on the initial microstructure. The sputtered MoS_2 coatings, like earlier burnished MoS_2 films, wore rapidly in sliding and rolling contact [4, 6-10]. More recently, coatings with dense, basal oriented microstructures have been produced via rf-sputtering [11], ion beam assisted deposition (IBAD) [12-14] and pulsed laser deposition (PLD) [15, 16]. However, wear studies of IBAD MoS_2 coatings [17, 18] determined that they, too, wore rapidly early in sliding life, despite their high endurance.

While processing advances enhanced MoS_2 coating microstructure and endurance, a number of other improvements in sputter deposited MoS_2 coatings were achieved through co-deposition with a variety of metals [7, 19, 20], laser alloying with Au [21], and multilayer deposition (alternating metals with MoS_2) [22, 23]. Increased crystallite size and density [19], lower friction [7, 20, 21], and retarded growth of edge oriented crystallites [22] were all observed. More recently several groups have demonstrated that coating endurance could be further improved by co-deposition of PbO [20, 24], Pb [25], or Ti [26] with MoS_2 using PLD, IBAD, and unbalanced magnetron processing, respectively. X-ray diffraction and Raman studies [24, 25, 27] showed that PbO and Pb alloying produced amorphous coatings, but that sliding transformed the surface to MoS_2. This was demonstrated conclusively by Dunn et al. using cross section high resolution transmission electron microscopy (HRTEM) [28].

At present, it is not understood why the amorphous films perform as well as (or even better than) the crystalline films. In this paper, we investigate the wear behavior of

amorphous Pb-Mo-S coatings. Optical microscopy and interferometry are used to characterize the worn surfaces' morphology and wear. Raman spectroscopy and cross section HRTEM are used to examine the coating structure and wear track surfaces. Results are discussed in terms of wear mechanisms at the nanometer and micron size scales and compared to previous results from unalloyed, crystalline MoS_2 coatings.

2. Experimental

Pb-Mo-S coatings were deposited by dual ion-beam deposition (IBD) in a vacuum chamber equipped with a Kaufman argon ion source; a full description of the IBD deposition process for these coatings is given elsewhere [25]. This process is considerably simpler than the IBAD counterpart used to produce MoS_2 coatings: no assist gun was used, and the deposition stage was not heated (a small temperature rise to ~60°C was observed during deposition). The coatings were deposited on various polished hardened steel substrates (M50, 52100, 440C and AMS 5749), as well as as-received, polished Si. Some of the coatings also had a thin (30-40 nm) TiN interlayer. Coatings contained between 4 and 26 at.% Pb; thicknesses ranged from 200 to 510 nm.

Friction and wear behavior of the coatings on steel were studied using the reciprocating sliding test methodology [17, 18] that we refer to as "stripe" testing. A schematic diagram of typical tracks resulting from stripe tests is shown in Fig. 1. Each track was run a length of 5 mm for the first n = {1,3,10,30,100,…} cycles, and then without lifting the ball, the stroke length was shortened to 3 mm for an additional 2n cycles; a new ball was used for each track. The resulting tracks each have 3 turnaround regions (or endpoints): one at each end of the track and another in between, from the shortened track length. Sliding tests were performed in dry air (RH <2%) using a ball-on-flat tribometer with 6.35 mm diameter 52100 steel balls, sliding speed of 4 mm s^{-1} and an initial load of 9.8 N (mean Hertzian pressure P_H = 0.92 GPa). Friction coefficients were monitored throughout the tests, and failure, if reached, was defined as the number of sliding cycles the coating endured before the average friction coefficient for a single cycle reached 0.2.

Reciprocating sliding tests were also performed on Pb-Mo-S coated Si substrates to allow preparation of HRTEM samples of wear track surfaces. However, in place of

stripe tests, 10 separate sliding tests (using a new ball for each test) were carried out, where each new track slightly overlapped the previous track. This procedure produced a wear scar ~1 mm wide, which ensured that the TEM analysis area would contain worn coatings surfaces. These tests were performed at similar sliding conditions to those described above; since the substrate was Si, the mean P_H was 0.82 GPa.

After sliding tests, wear tracks on the coatings and transfer films on the balls were examined optically by interference (Nomarski) microscopy. Coating wear track depths (to within 10 nm) were determined using Michelson interferometry. Micro-Raman spectroscopy of ball transfer films was performed using a Renishaw imaging microscope equipped with a low-power (~25 mW) Ar^+ laser (514 nm) with 1 cm^{-1} spectrometer resolution and 2 μm spatial resolution at the sample surface. Cross-section HRTEM samples were made from the wear tracks on Si samples via standard techniques. Samples were cleaved normal to the wear track plane and glued together with a two-part epoxy, then mechanically thinned, dimpled, and ion milled with 5.0 keV Ar^+ ions until perforation. Cross-sections were made in both the longitudinal (along the sliding direction) and transverse (across the width of the track) directions. Wear track cross-sections were examined using a Hitachi H-9000 operated at 300 keV in bright-field (BF) imaging and selected area electron diffraction (SAED) modes.

3. Results

3.1 Coating friction and wear depths

Friction coefficients were high during the first several passes (>0.1), but dropped below 0.05 by 10 to 100 cycles (depending on the particular coating) and were similar to those we reported previously [25]. Figure 2a shows wear track depths as a function of reciprocating sliding cycle from tests performed on Pb-Mo-S coatings with four different thicknesses; to more clearly display changes in wear depths before 10000 cycles, a semi-log plot of the wear data is shown in Fig. 2b. No measurable wear was detected before 100 cycles for any of the coatings; two coatings didn't have measurable wear until 1000 to 3000 sliding cycles. By 1000 cycles, cumulative wear rates were below 0.07 nm/cycle, and less than 0.005 nm/cycle by 10000 cycles. Total wear for all of the coatings was low up to 30000 cycles: none were worn more than 50% of the original coating thickness, and

all but two of the many sliding tests resulted in less than 100 nm coating wear in the tracks. Remarkably, the 500 nm thick coating exhibited a wear depth of only 40 nm by 32000 cycles.

3.2. Wear scar analyses

3.2.1. Optical analyses of coating wear tracks and ball transfer films

All wear tracks and ball transfer films were examined optically. Evolution of wear track and ball transfer films was qualitatively similar for the four coatings; micrographs from the 300 nm thick coating are representative of their behavior.

Optical micrographs of typical worn track surfaces (from the 300 nm coating) are shown in Fig. 3, along with representative interferometry profiles. Between 1 and 100 cycles (Fig. 3a), tracks were nearly invisible and could only be identified by slight burnishing of the coating and an occasional debris particle. No wear could be seen in the track profile. By 300 to 3000 cycles (Fig. 3b), narrow, shallow scratches were seen in the micrograph as well as in the interferometry profile. Some scratches were up to 50 nm deep. Small, loose debris particles were found along the sides and at the ends of the tracks, increasing in quantity as sliding progressed. By 9000 cycles (Fig. 3c), scratches were more pronounced, and a noticeable furrow (~50 nm deep) was observed on the track. Redeposited wear debris was found in the track, and loose debris along the sides and at ends of the track. Between 40000 and 60000 cycles (Fig. 3d), centers of wear tracks appeared roughened. Copious amounts of fine debris particles lined the track sides and ends.

Turnaround regions of the wear tracks (at either end, and one in the middle from the shorter portion of the track, as diagrammed in Fig. 1) were also examined. An example from a middle turnaround point for the 300/900 cycle track is shown in Fig. 4. In regions directly under the ball turnaround region, no significant buildup of redeposited debris was observed in any of the wear tracks. Piles of fine wear debris particles were observed beyond the turnaround points at track ends beyond 100 sliding cycles, increasing in quantity as sliding progressed. As can be seen in Fig. 4, scratches seen on the right side of the track (after 300 cycles) were unchanged after 600 additional sliding cycles. The similarity of the scratches between 300 and 900 cycles suggests that scratching was a discrete event and occurred infrequently.

The evolution of the ball transfer films formed on 52100 steel from 9 to 40000 cycles is shown in Fig. 5a-d. Virtually no visible material transfer could be found between 1 and 30 passes (Fig. 5a). By 90 cycles, a small amount of transfer material was observed around the edges of the contact zone; the center of the contact zone remained smooth in appearance. By 300 cycles (Fig. 5b) a smooth, continuous film formed over the ball surface, with thicker debris pads at the edges of the contact zone. The transfer film appearance is similar at 900 cycles. Some fine particles were observed on the ball surface close to the contact zone. As sliding progressed, the smooth transfer film increased in size (Fig. 5c) and more fine particulate debris were scattered around the contact. Ball transfer films at 40,000 to 60,000 cycles (Fig. 5d) exhibited thick transfer films with copious fine debris particles distributed over the ball surface outside the contact zone.

3.2.2. Micro-Raman spectroscopy of worn surfaces

Raman analysis was performed on wear tracks. Burnished areas usually showed spectra of the as-deposited coating; however, in some locations, bands consistent with crystalline MoS_2 [29] were seen after as few as 100 cycles. Some debris particles showed spectra similar to as-deposited coating and some, to the MoS_2 bands, while others fluoresced strongly. Examples of spectra from inside a 3000 cycle track, along with as-deposited coating, are shown in Fig. 6.

Figure 7 shows Raman spectra from 9, 300 and 9000 cycle ball wear scars previously presented in Figure 5. Ball wear scars exhibited the MoS_2 bands inside and outside the contact zone. Most importantly, the bands were found inside the contact zone after only 9 cycles. This demonstrates that a thin transfer film, although transparent, was present in the ball contact and suggests that the transfer film had transformed from amorphous to crystalline MoS_2 by 9 cycles. Not all regions on the ball wear scars showed MoS_2: like the wear tracks, some locations inside and outside the ball contact zone exhibited Raman spectra similar to the as deposited coating or fluoresced (Fig. 6). No evidence for Mo or Pb oxidation products (MoO_2, MoO_3 or $PbMoO_4$) was found.

3.2.3. TEM analyses of wear scar cross sections

Cross-section HRTEM was performed on tracks worn in a 200 nm coating deposited on Si. Figure 8 shows a 100 cycle Pb-Mo-S wear track; the sliding direction is perpendicular to the plane of the image. The interface between the lighter epoxy region

(upper half) and darker Pb-Mo-S (lower half) is the wear track surface. Below the wear track surface, the microstructure of the Pb-Mo-S coating remained unchanged from the as-deposited microstructure (e.g. amorphous), showing no long range order via HRTEM [28] and consistent with previous x-ray diffraction and micro-Raman spectroscopy studies [25]. Horizontal fringes ~5-10 nm long were observed at the wear track surface; an example is marked in the image between arrows. The spacing between fringes for this patch is ~ 0.65 nm; fringe spacing of other patches ranged up to 0.70 nm.

Figure 9 is a HRTEM image of a portion of the Pb-Mo-S track after 1000 cycles; the sliding direction, in this case, is parallel to the image plane. At the track surface is a crystalline layer, 2 to 4 fringes thick; arrows mark an area where a segment of the layer has been pulled away from the surface. In addition, fringes ~3-5 nm long can be seen below the sliding surface and are marked by the letter "s". As in the 100 cycle track, the subsurface Pb-Mo-S remained amorphous. In other regions of the 1000 cycle track (not shown), crystalline debris (10-12 nm thick) was found on top of the horizontal fringes at the wear track surface [28].

Spacings between the layers observed in the HRTEM images are somewhat greater than that between basal planes of molybdenite (0.615 nm) [30], but are consistent with the basal plane spacings found in MoS_2 films deposited by rf-sputtering [31] and ion-beam assisted deposition (IBAD) [32, 33]. The layers, then, are consistent with basal-oriented MoS_2.

4. Discussion

Wear scar analysis of steel sliding against Pb-Mo-S coatings in dry air revealed both nanometer scale and micrometer scale processes associated with wear. HRTEM studies of the wear tracks gave direct evidence that low speed, high stress sliding — a tribomechanical process — can convert amorphous Pb-Mo-S into crystalline MoS_2. The transformation, previously inferred from Raman spectroscopy of wear scars on Pb-O-Mo-S [24] and Pb-Mo-S [25] alloys, has now been verified. Moreover, HRTEM shows that the transformation occurs by creating basal-oriented layers at the outermost layers of the track. An extended discussion of the transformation is given elsewhere[28].

HRTEM images also give evidence, for the first time, that wear of MoS_2 can take place layer-by-layer at the atomic level. Fig. 9 shows a basal-oriented S-Mo-S layer "lifting" off another S-Mo-S layer at the weak (van der Waals) interface. The layers are removed from the wear track surface and transferred to the ball surface, as demonstrated by Raman spectroscopy in Fig. 7. The transformation, and removal, of MoS_2 layers occurred after as few as 9 sliding cycles. The removal of layers of MoS_2 can be explained by the lack of strong bonding between S-Mo-S layers, which are easily sheared and/or removed.

On a micrometer scale, narrow scratches (Fig. 3b) and corresponding lumps of debris on ball surfaces and at track ends (Fig. 4) indicate a plowing wear mechanism. Debris showing featureless Raman spectra (as in the as-deposited coating) are also consistent with plowing wear. While we don't know what causes plowing events, they are important, but infrequent, events in the sliding process. As shown in Fig. 4, no new scratches are observed even though 600 cycles had elapsed between the left and right portions shown on the wear tracks. Moreover, scratches did not heal or fill in during sliding.

The percentage of coating worn for the Pb-Mo-S coatings was calculated from the wear depth and coating thickness data and is plotted in Fig. 10. None of the four coatings showed more than 25% coating loss by 10000 cycles. No distinct rapid wear region was identifiable in the plots or by morphological changes on worn surfaces. The low wear of these coatings is consistent with layer-by-layer removal of MoS_2 crystallites and infrequent, shallow plowing events. This wear behavior is in sharp contrast to that observed under identical sliding conditions for crystalline IBAD MoS_2 coatings: no wear could be measured during the first 100 cycles, but rapid wear (loss of 50 to 80% of coating thickness) occurred between 100 and 1000 cycles [17, 18]. Rapid wear during the early stages of sliding and rolling is typical of crystalline MoS_2 [4, 6-10]. Rapid wear of sputtered MoS_2 may result from fracture of crystallites [7] and can be influenced by initial microstructure [6]. Subsurface crack formation and subsequent delamination of large flakes of coating has been observed in some dense MoS_2 coatings [34, 35] but has not been observed for IBAD MoS_2 coatings [36]. None of these fracture behaviors was seen in the Pb-Mo-S coatings, either at the micrometer or nanometer scale.

It is not clear why the Pb-Mo-S coatings resist the rapid wear seen in MoS_2. A microstructure devoid of MoS_2 planes in the bulk might explain the low wear rate of Pb-Mo-S coatings, especially if this microstructure hinders fracture within the coating. However, we have examined dense, basal oriented IBAD MoS_2 coatings amorphized by ion-irradiation and found that the amorphized MoS_2 coatings wore more rapidly than the crystalline IBAD MoS_2 parent coatings [37]. Thus, the amorphous nature of the Pb-Mo-S coatings does not necessarily explain their wear resistance.

Can the wear resistance (and endurance) of the Pb-Mo-S be explained by the third body processes responsible for the long life and low friction of IBAD MoS_2? [17, 18] Both Pb-Mo-S and IBAD MoS_2 produced transfer films on the uncoated ball, which accounts for low friction coefficient throughout sliding life; moreover, both generated loose debris as the coating wore. However, debris from MoS_2 coatings built up reservoirs of MoS_2 which resupplied lubricant to the rapidly wearing track. This replenishment accounted for the long endurance, given that most of the coating was lost from the wear track during the first 10% of sliding life. In contrast, debris from Pb-Mo-S coatings were, for the most part, ejected from the sliding contact. Buildup of redeposited debris was minimal, and healing or filling in of scratches was not observed; all of these limited third body participation in a resupply process. On the other hand, the limited amount and size of debris generated may be advantageous for bearing environments where torque bumps and debris generation are known to contribute to performance problems [38].

Therefore, third body processes for the Pb-Mo-S coatings are not as important to endurance as for IBAD MoS_2. Instead, we attribute the high endurance of the Pb-Mo-S coatings simply to slow wear of the coating. Transformation of surface Pb-Mo-S to MoS_2 layers, and subsequent transfer of MoS_2 to ball surfaces, provided an easily sheared interface. Since these low shear strength interfaces were only found at or near the coating surface, just one or several layers were lost at a time. This, plus the low occurrence of plowing events, accounts for the low wear rates (and hence high endurance) observed.

Several issues remain unanswered by the present study. First, what is the role of Pb in the wear resistance of these coatings? Second, are the transfer films and wear debris generated in sliding against Pb-Mo-S coatings more benign than those formed from contacts with crystalline MoS_2 coatings? Maybe Pb-Mo-S wears more slowly because the

microstructures are not susceptible to delamination. Alternately, perhaps increased adhesion of transfer material to the ball surfaces due to the presence of Pb may play a role in preventing coating damage.

5. Conclusions

Pb-Mo-S coatings were found to be remarkably wear resistant. Two wear mechanisms were identified: layer-by-layer removal of MoS_2 and plowing. At the nanometer scale, wear proceeded in a two-part process: transformation of the coating surface to MoS_2, then layer-by-layer removal of MoS_2. This process was observed by as few as 9 sliding cycles, where Raman microscopy detected MoS_2 in an optically transparent transfer film. Wear of the Pb-Mo-S coatings also occurred, on a microscopic scale, by plowing processes. The long endurance of the Pb-Mo-S coatings was attributed to slow wear of the coatings, with redistribution processes playing a minor role as compared to MoS_2 coatings.

Acknowledgements

The authors thank R.N. Bolster for coating deposition, A. Kyriakopoulos and J.C. Wegand for contributing to the wear testing, as well as L.E. Seitzman and A. Erdemir for useful discussions. Work was performed while D.N.D. was supported by an ONR/ASEE post doctoral associateship. The work was supported by the Office of Naval Research.

References

[1] T. Spalvins, A review of recent advances in solid film lubrication, *Journal of Vacuum Science and Technology A, 5* (1987) 212-219.

[2] T. Spalvins, Morphological and frictional behavior of sputtered MoS_2 films, *Thin Solid Films, 96* (1982) 17-24.

[3] V. Buck, Lattice parameters of sputtered MoS_2 films, *Thin Solid Films, 198* (1991) 157-167.

[4] P.D. Fleischauer and R. Bauer, Chemical and Structural Effects on the Lubrication Properties of Sputtered MoS_2 Films, *Tribol. Trans., 31* (1988) 239-250.

[5] M.R. Hilton and P.D. Fleischauer , Structural Studies of Sputter-Deposited MoS_2 Solid Lubricant Films, in L. Pope, L. Fehrenbacher, and W. Winer, (eds.) , *New Materials Approaches to Tribology: Theory and Applications*.: Mater. Res. Soc. Proc., Vol. 140, Materials Research Society, 1989, pp. 227-238.

[6] M.R. Hilton, R. Bauer, and P.D. Fleischauer, Tribological Performance and Deformation of Sputter-Deposited MoS_2 Solid Lubricant Films during Sliding Wear and Indentation Contact, *Thin Solid Films, 188* (1990) 219-236.

[7] T. Spalvins, Frictional and Morphological Properties of Au-MoS_2 Films Sputtered from a Compact Target, *Thin Solid Films, 118* (1984) 375-384.

[8] G.D. Gamulya, G.V. Dobrovol'skaya, I.L. Lebedeva, and T.P. Yukhno, General Regularities of Wear in Vacuum for Solid Film Lubricants Formulated with Lamellar Materials, *Wear, 93* (1984) 319-332.

[9] I.L. Singer, S. Fayeulle, and P.D. Ehni, Wear behavior of triode-sputtered MoS_2 coatings in dry sliding contact with steel and ceramics, *Wear, 195* (1996) 7-20.

[10] G.B. Hopple, J.E. Keem, and S.H. Loewenthal, Development of fracture resistant, multilayer films for precision ball bearings, *Wear, 162-164* (1993) 919-924.

[11] J. Moser, F. Lévy, and F. Bussy, Composition and growth mode of MoS_x sputtered films, *Journal of Vacuum Science and Technology A, 12* (1994) 494-500.

[12] H. Kuwano and K. Nagai, Friction-reducing coatings by dual fast atom beam technique, *Journal of Vacuum Science and Technology A, 4* (1986) 2993-2996.

[13] R.N. Bolster, I.L. Singer, J.C. Wegand, S. Fayeulle, and C.R. Gossett, Preparation by ion-beam-assisted deposition, analysis and tribological behavior of MoS_2 films, *Surf. Coat. Technol., 46* (1991) 207-216.

[14] L.E. Seitzman, I.L. Singer, and R.N. Bolster, Effects of Temperature and Ion-to-Atom Ratio on the Orientation of IBAD MoS_2 Coatings, *Thin Solid Films, 260* (1995) 143-147.

[15] M.S. Donley, P.T. Murray, and N.T. McDevitt , Synthesis and characterization of MoS_2 thin films grown by pulsed laser evaporation, in L.E. Pope, L.L. Fehrenbacher, and W.O. Winer, (eds.) , *New Materials Approaches to Tribology: Theory and Applications*, Vol. 140, Materials Research Society, Pittsburgh, PA, 1989, pp. 277-282.

[16] J.S. Zabinski, M.S. Donley, P.J. John, V.J. Dyhouse, A.J. Safriet, and N.T. McDevitt , Crystallization of molybdenum disulfide films deposited by pulsed laser ablation, in H.A. Atwater, F.A. Houle, and D.H. Lowndes, (eds.) , *Surface Chemistry and Beam-Solid Interactions*, Vol. 201, Materials Research Society, Pittsburgh, PA, 1991, pp. 195-200.

[17] K.J. Wahl and I.L. Singer, Quantification of a lubricant transfer process that enhances the sliding life of a MoS_2 coating, *Tribol. Lets., 1* (1995) 59-66.

[18] K.J. Wahl and I.L. Singer , Role of the Third Body in Life Enhancement of MoS_2, in D. Dowson, *et al.*, (eds.) , *The Third Body Concept: Interpretation of Tribological Phenomena*, Vol. 31, Elsevier, Amsterdam, 1996, pp. 407-413.

[19] B.C. Stupp, Synergistic Effects of Metals Co-Sputtered with MoS_2, *Thin Solid Films, 84* (1981) 257-266.

[20] J.S. Zabinski, M.S. Donley, S.D. Walck, T.R. Schneider, and N.T. McDevitt, The Effects of Dopants on the Chemistry and Tribology of Sputter-Deposited MoS_2 Films, *Tribol. Trans., 38* (1995) 894-904.

[21] L.E. Pope, T.R. Jervis, and M. Nastasi, Effects of laser processing and doping on the lubrication and chemical-properties of thin MoS_2 films, *Surf. Coat. Technol., 42* (1990) 217-225.

[22] M.R. Hilton, R. Bauer, S.V. Didziulis, M.T. Dugger, J.M. Keem, and J. Scholhamer, Structural and tribological studies of MoS_2 solid lubricant films having tailored metal-multilayer nanostructures, *Surface Coatings Technology, 53* (1992) 13-23.

[23] S. Mikhailov, A. Savan, E. Pflüger, L. Knoblauch, R. Hauert, M. Simmonds, and H. Van Swygenhoven, Morphology and tribological properties of metal(oxide)-MoS_2 nanostructured multilayer coatings, *Surf. Coat. Technol., 105* (1998) 175-183.

[24] J.S. Zabinski, M.S. Donley, V.J. Dyhouse, and N.T. McDevitt, Chemical and Tribological Characterization of PbO-MoS_2 Films Grown by Pulsed Laser Deposition, *Thin Solid Films, 214* (1992) 156-163.

[25] K.J. Wahl, L.E. Seitzman, R.N. Bolster, and I.L. Singer, Low friction, high-endurance, ion-beam-deposited Pb-Mo-S coatings, *Surf. Coat. Technol., 73* (1995) 152-159.

[26] D.G. Teer, J. Hampshire, V. Fox, and V. Bellido-Gonzalez, The tribological properties of MoS_2/metal composite coatings deposited by closed field magnetron sputtering, *Surf. Coat. Technol., 94-95* (1997) 572-577.

[27] N.T. McDevitt, M.S. Donley, and J.S. Zabinski, Utilization of Raman spectroscopy in tribochemistry studies, *Wear, 166* (1993) 65-72.

[28] D.N. Dunn, K.J. Wahl, and I.L. Singer , Nanostructural Aspects of Wear Behavior in Ion-Beam Deposited MoS_2 and Pb-Mo-S Films, in N.R. Moody, W.W. Gerberich, S.P. Baker, and N.A. Burnham, (eds.), *Fundamentals of Nanoindentation and Nanotribology*, Vol. 522, Materials Research Society, Pittsburgh, PA, 1998, pp. 451-456.

[29] T.J. Weiting and J.L. Verble, Infrared and Raman Studies of Long-Wavelength Optical Phonons in Hexagonal MoS_2, *Phys. Rev. B, 3* (1971) 4286-4292.

[30] J.C.P.D.S., Powder Diffraction File, International Center for Diffraction Data, Swarthmore, Pa, 1987, Card 37-1492.

[31] J.R. Lince and P.D. Fleischauer, Crystallinity of Rf-Sputtered MoS_2 Films, *J. Mater. Res., 2* (1987) 827-838.

[32] L.E. Seitzman, R.N. Bolster, and I.L. Singer, X-ray diffraction of MoS_2 coatings prepared by ion-beam-assisted deposition, *Surf. Coat. Technol., 52* (1992) 93-98.

[33] D.N. Dunn, L.E. Seitzman, and I.L. Singer, MoS_2 Deposited by Ion Beam Assisted Deposition: 2H or Random Layer Structure?, *J. Mater. Res., 13* (1998) 3001-3007.

[34] J.L. Grosseau-Poussard, H. Garem, and P. Moine, High-Resolution Transmission Electron Microscopy Study of Quasi-Amorphous MoS_x Coatings, *Surf. Coat. Technol., 78* (1996) 19-25.

[35] J. Moser and F. Lévy, MoS_{2-x} lubricating films: structure and wear mechanisms investigated by cross-sectional transmission electron microscopy, *Thin Solid Films, 228* (1993) 257-260.

[36] D.N. Dunn, K.J. Wahl, and I.L. Singer, Nanostructural Aspects of Wear Behavior of IBAD MoS_2, in preparation.

[37] K.J. Wahl, D.N. Dunn, and I.L. Singer , Effects of Ion-Implantation on Endurance and Wear Behavior of IBAD MoS_2, in preparation.

[38] R. Bauer and P.D. Fleischauer, Torque Characteristics of Solid-Lubricated Precision Bearings During Oscillitory Motion, *Tribol. Trans., 38* (1995) 1-10.

Figure Captions

Fig. 1. Schematic diagram of reciprocating sliding "stripe" testing series for this wear study. Arrow marked "start" indicates test starting location, turnaround points are indicated by open circles, and sliding cycles for the track segments are numbered.

Fig. 2. Pb-Mo-S coating wear track depths measured by interference microscopy plotted on a (a) linear and (b) log scale.

Fig. 3. Optical micrographs and interferometry profiles of Pb-Mo-S wear tracks after (a) 100, (b) 1000, (c) 9000, and (d) 40000 sliding cycles.

Fig. 4. Wear track segments run to 900 (left side) and 300 (right side) reciprocating sliding cycles at the middle turnaround region of the wear track. Two scratches are evident by 300 cycles, and are not found to be measurably deeper or increased in number after 600 additional cycles. The debris at the center of the micrograph was ejected at the end of the shortened section (900 cycles) of the wear track.

Fig. 5. Optical micrographs of ball transfer films after (a) 9, (b) 300, (c) 9000 and (d) 40000 cycles against Pb-Mo-S coating.

Fig 6. Micro-Raman spectra of as-deposited coating as well as different regions of Pb-Mo-S wear track surfaces and ball transfer films after 3000 sliding cycles.

Fig. 7. Micro-Raman spectra of ball transfer films formed after sliding against Pb-Mo-S coatings for 9, 300, and 9000 cycles.

Fig. 8. Cross-section HRTEM micrograph of Pb-Mo-S wear track surface after 100 cycles (sliding direction along epoxy-Pb-Mo-S interface, normal to the image plane). The Pb-Mo-S coating remains largely unchanged except for small patches of transformed MoS_2 at the sliding interface.

Fig 9. Cross-section HRTEM micrograph of Pb-Mo-S wear track surface after 1000 cycles (sliding direction parallel to image plane). To the left and marked with arrows is a region where two basal planes of MoS_2 have been pulled up. Also, subsurface patches of MoS_2 are marked by the letter "s".

Fig 10. Pb-Mo-S coating wear track depths from Fig. 2 plotted as percent of coating worn.

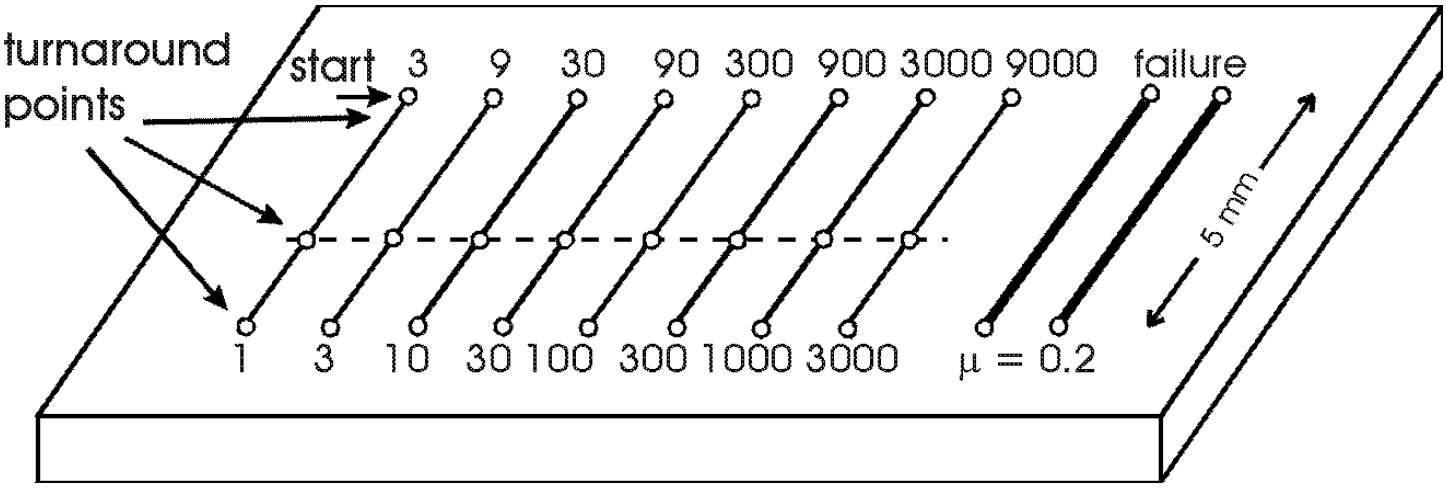

Figure 1. Schematic of reciprocating sliding ‘stripe’ testing series for this wear study. Arrow marked “start” indicates test starting location, turnaround points are indicated by open circles, and sliding cycles for the track segments are numbered.

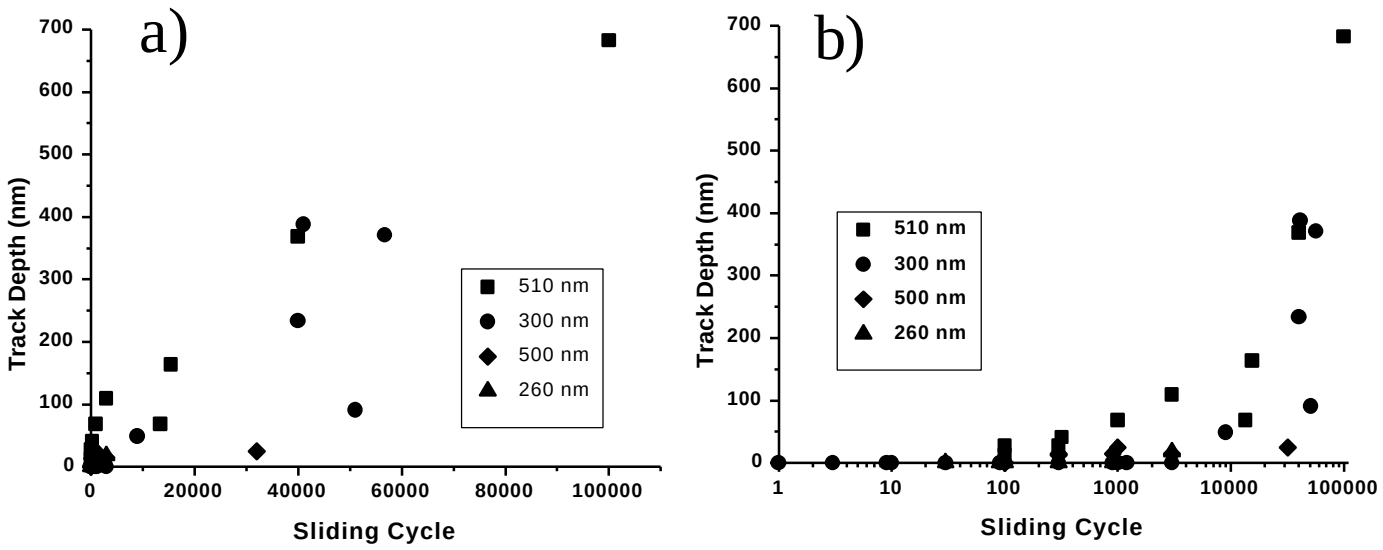

Figure 2. Pb-Mo-S coating wear track depths measured by interference microscopy plotted on (a) linear and (b) semi-log scales.

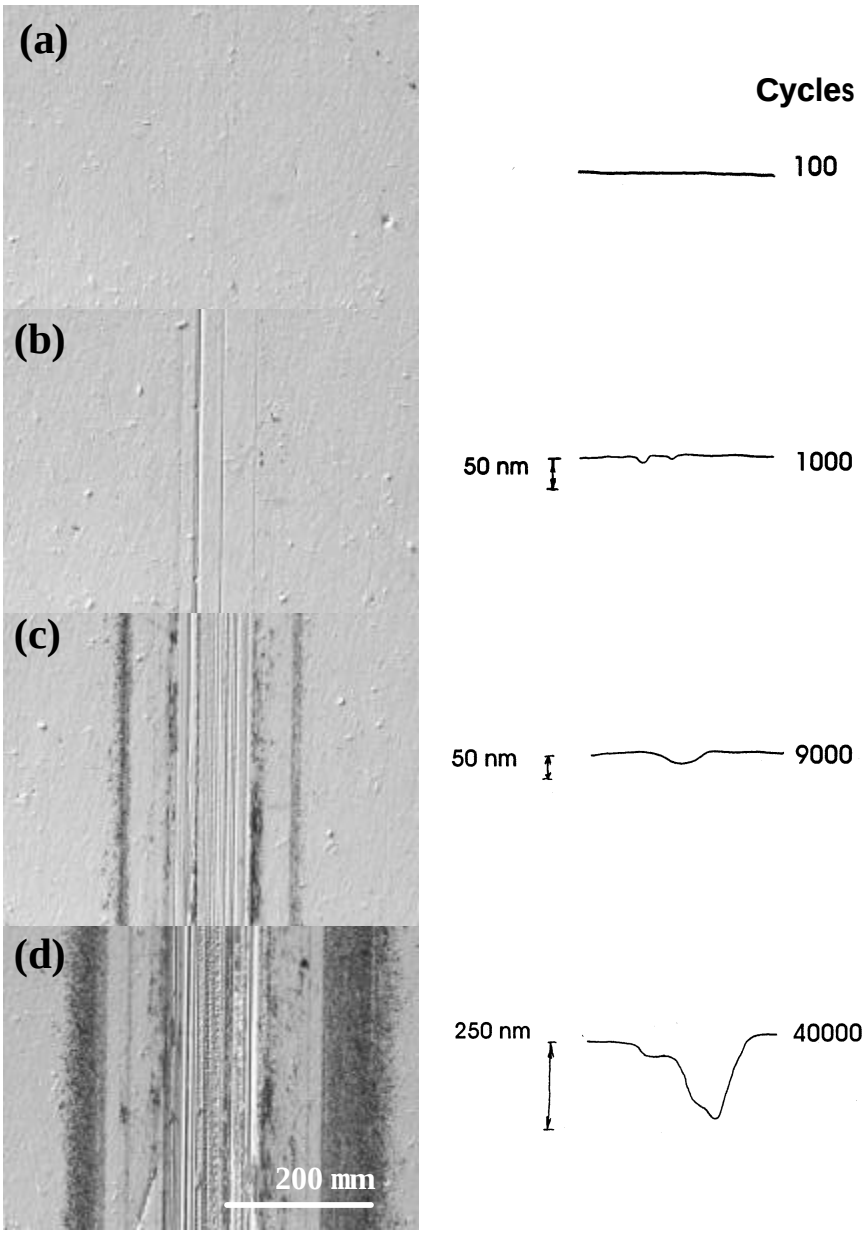

Figure 3. Optical micrographs and interference microscopy profiles of IBD Pb-Mo-S wear tracks worn to (a) 100, (b) 1000, (c) 9000, and (d) 40000 reciprocating sliding cycles in dry air.

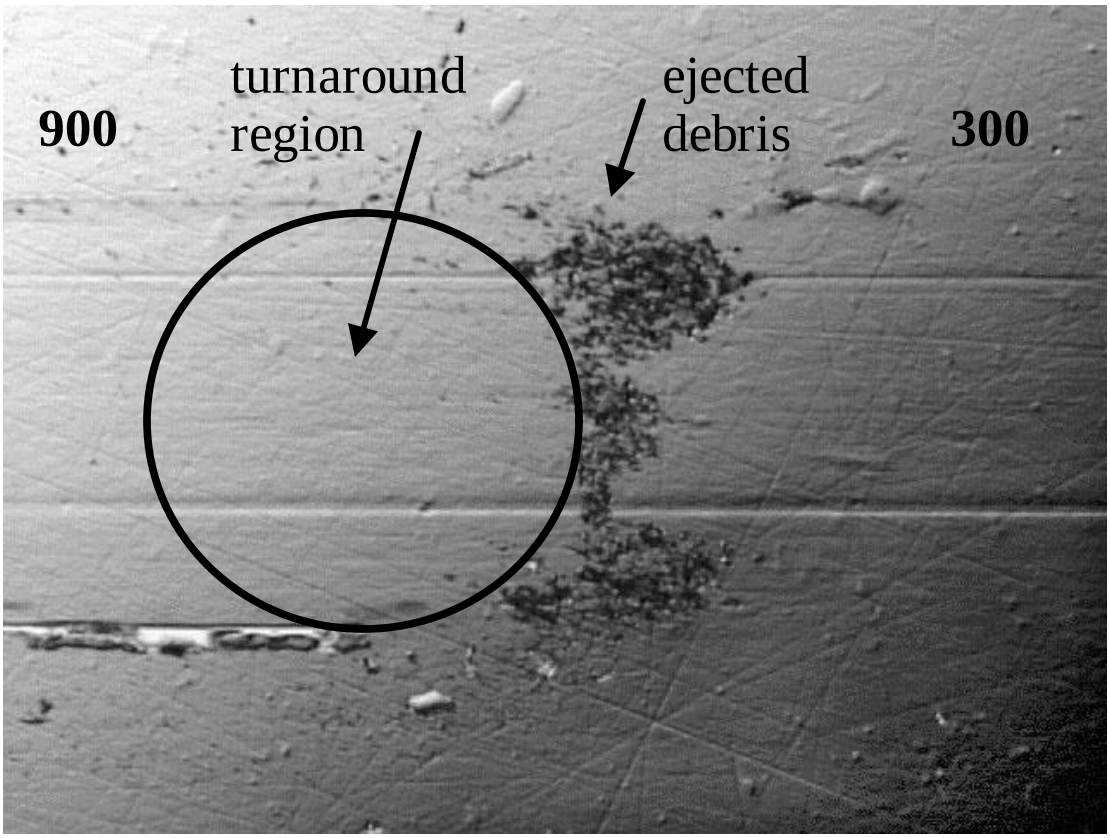

Figure 4. Wear track segments run to 900 (left side) and 300 (right side) reciprocating sliding cycles at the center turnaround region of the wear track. Two scratches are evident by 300 cycles, and are not found to be measurably deeper or increased in number after 600 additional sliding cycles. The debris at the center of the micrograph was ejected at the end of the shortened section (900 cycles) of the wear track.

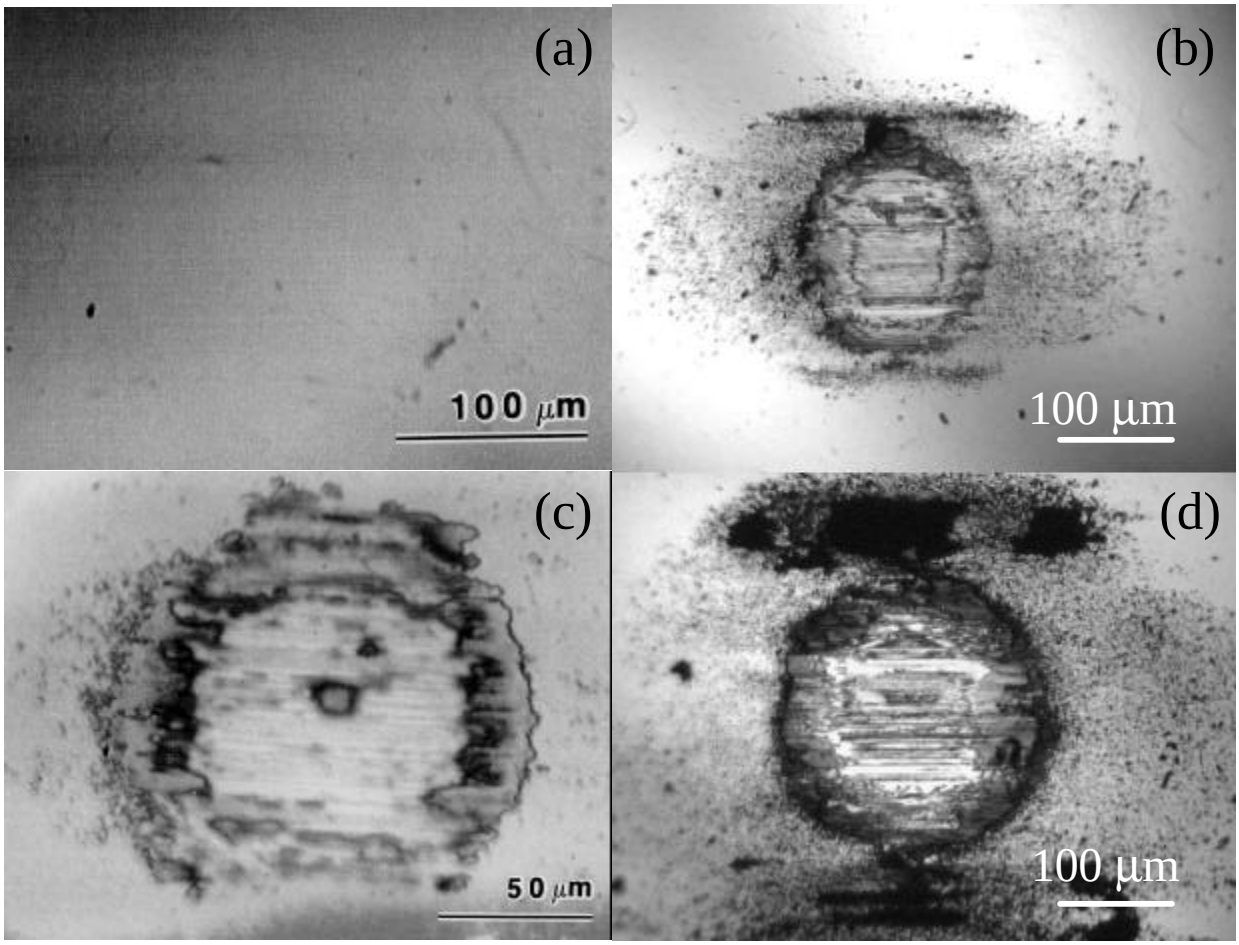

Figure 5. Optical micrographs of ball transfer films after (a) 9, (b) 300, (c) 9000 and (d) 40000 cycles against Pb-Mo-S coating.

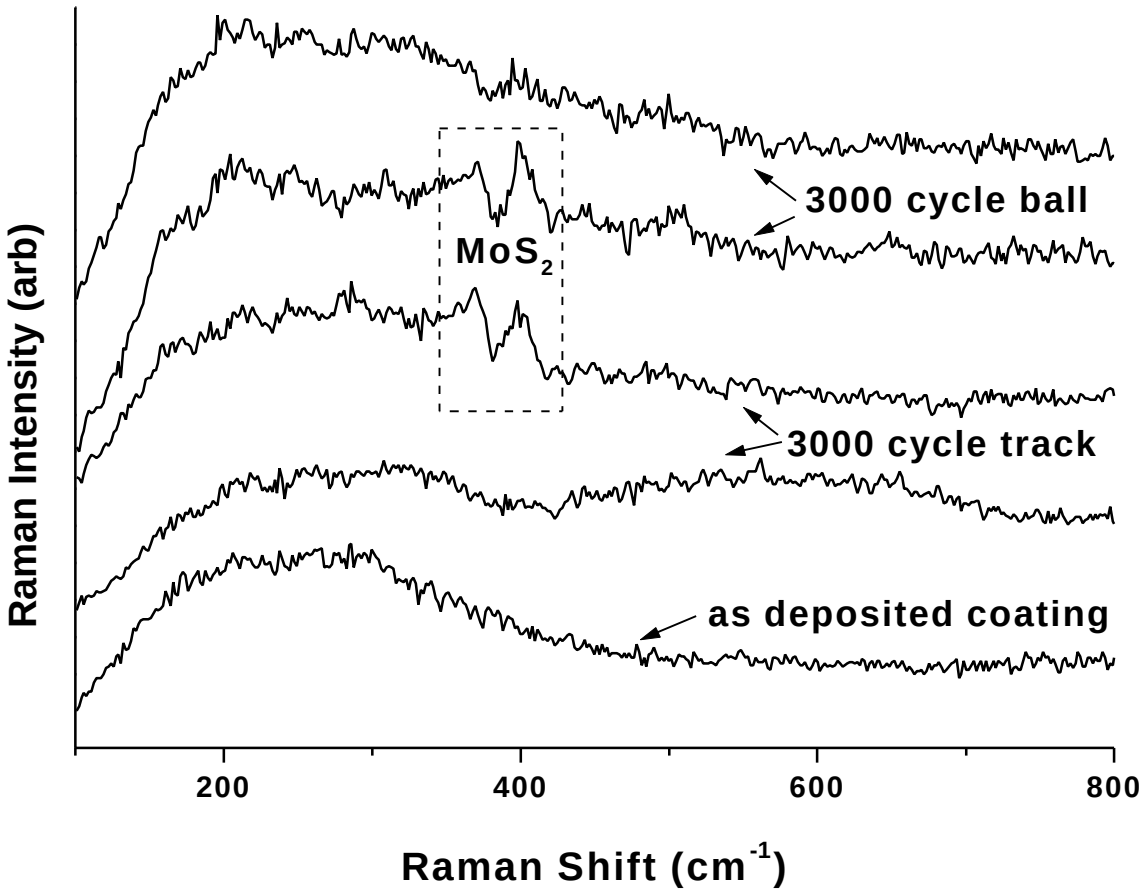

Figure 6. Micro-Raman spectra of as-deposited coating as well as different regions of Pb-Mo-S wear track surfaces and ball transfer films after 3000 sliding cycles.

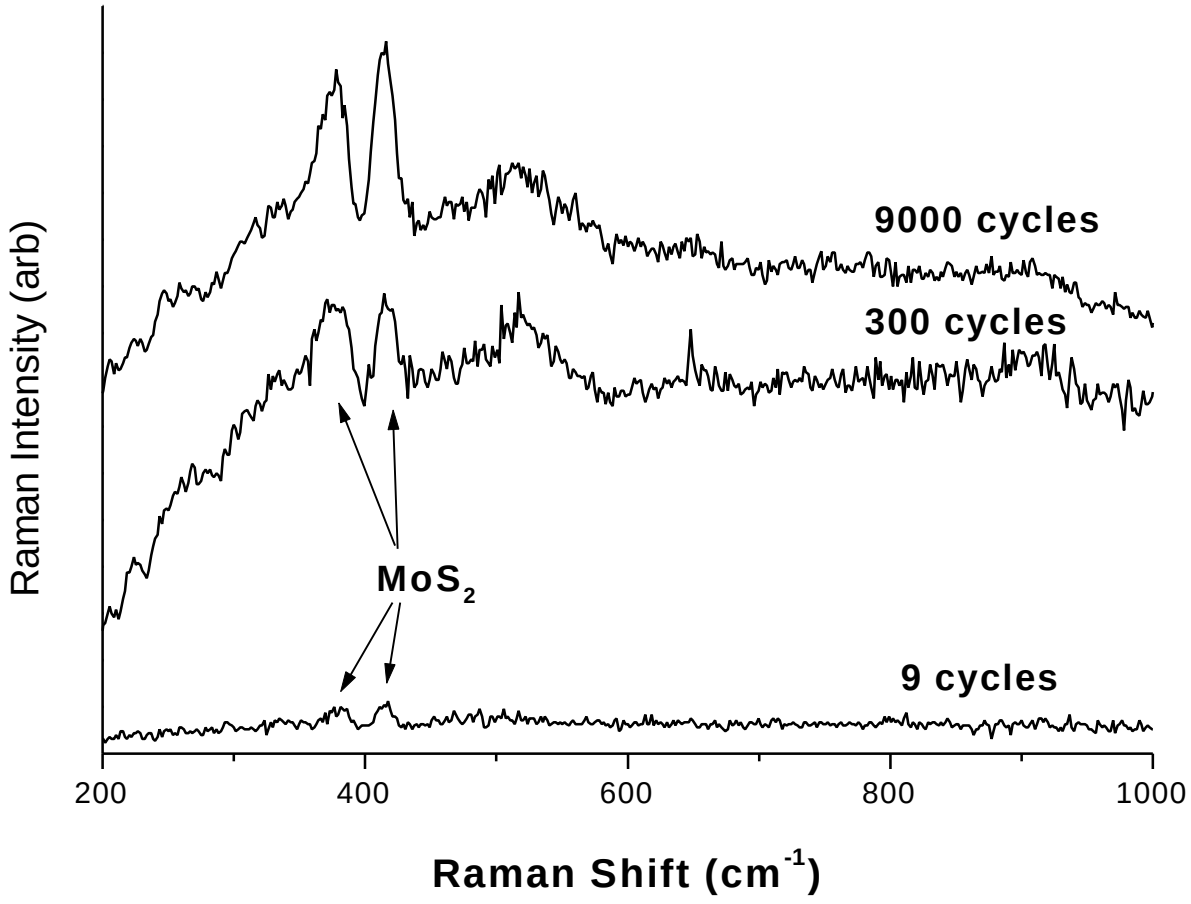

Figure 7. Micro-Raman spectra of ball transfer films formed after sliding against Pb-Mo-S coating for 9, 300, and 9000 cycles.

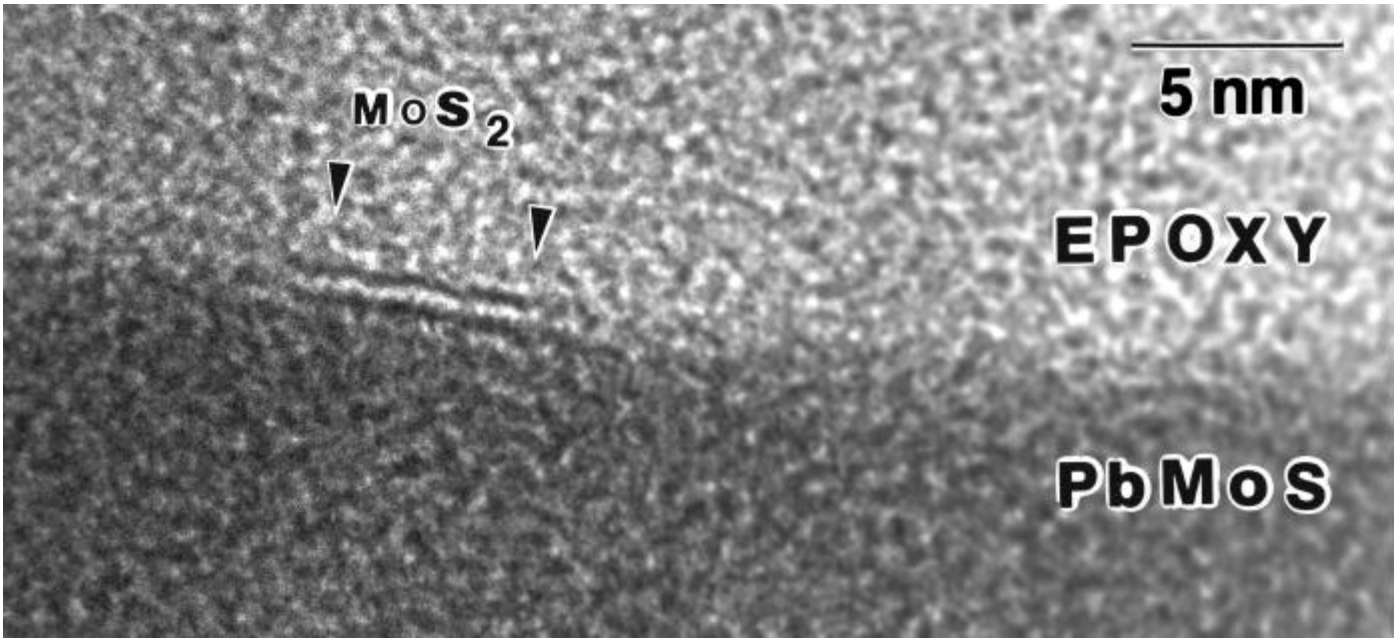

Figure 8. Cross-section HRTEM micrograph of Pb-Mo-S wear track surface after 100 sliding cycles (sliding direction along epoxy-Pb-Mo-S interface, normal to the image plane). ThePb-Mo-S coating remains largely unchanged except for small patches of transformed MoS_2 at the sliding interface (between arrows).

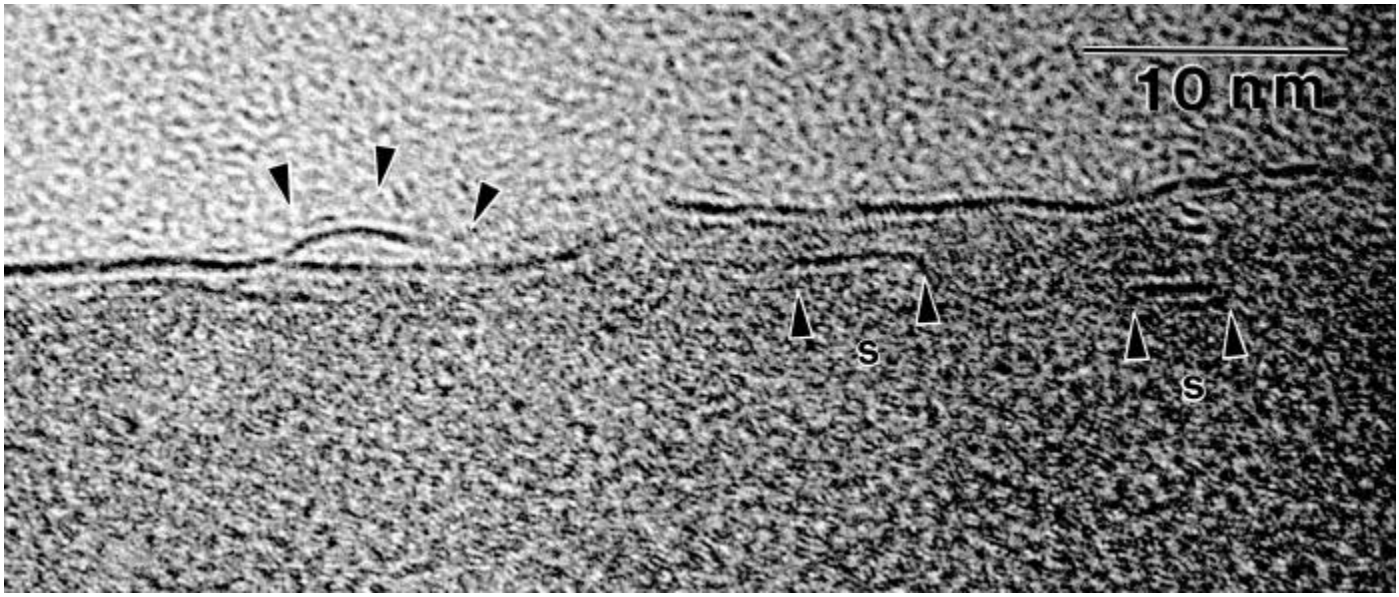

Figure 9. Cross section HRTEM micrograph of Pb-Mo-S wear track surface after 1000 sliding cycles (sliding direction parallel to image plane). To the left and marked with arrows is a region where two basal planes of MoS_2 have been pulled up. Also, subsurface patches of MoS_2 are marked by the letter “s”.

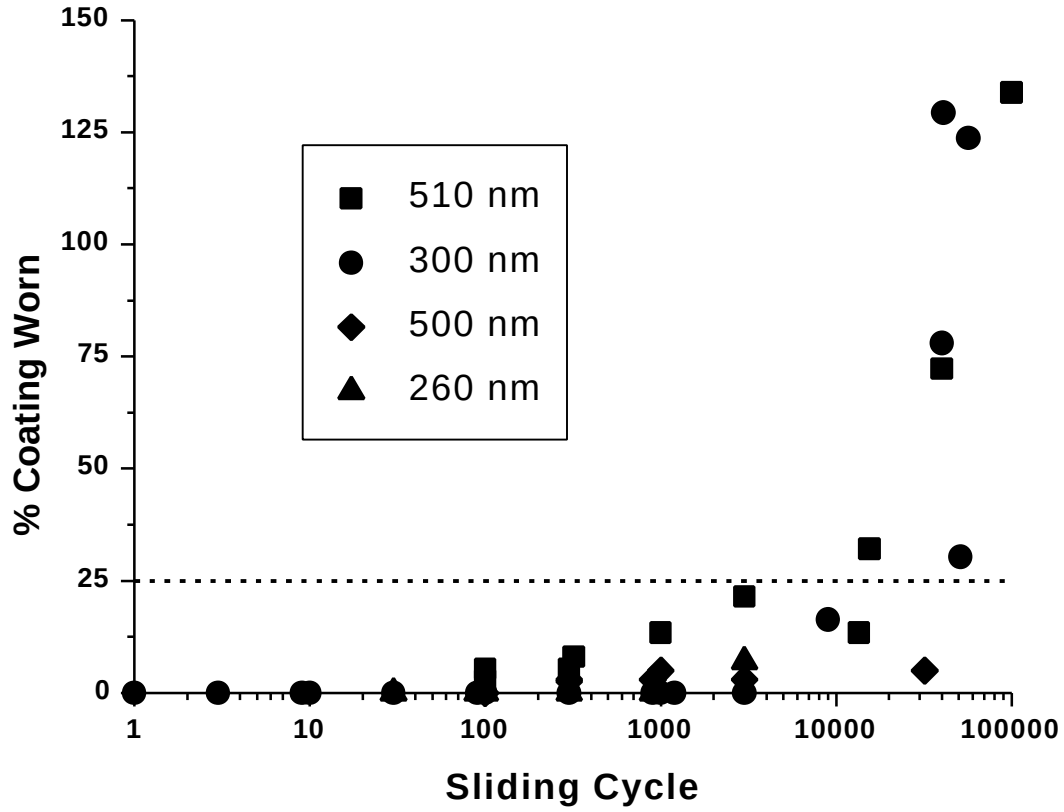

Fig. 10. Pb-Mo-S track depths from Fig. 2 plotted as percent of coating worn.